Electric-field-induced reorientation and flip in domain magnetization and light diffraction in an yttrium-iron-garnet/lead-zirconate-titanate bilayer

I. V. Zavislyak,[1] V. P. Sohatsky,[1] M. A. Popov,[1] and G. Srinivasan[2]
[1]*Radiophysics Department, Taras Shevchenko National University of Kyiv, Kyiv 01601, Ukraine*
[2]*Physics Department, Oakland University, Rochester, Michigan 48309, USA*
(Received 23 November 2012; revised manuscript received 21 January 2013; published 22 April 2013)

A continuous reorientation and an abrupt flip to a canted structure in the magnetization of stripe domains are observed under the influence of an electric field in an yttrium-iron-garnet (YIG)/lead-zirconate-titanate (PZT) bilayer. Magneto-optic techniques have been utilized for the observation of the domain structure and the magnetization flip. It is found that electrically generated mechanical stress in PZT induces an uniaxial anisotropy field in YIG, which is large enough to initially cause a gradual change in the domain magnetization and then a transition from out-of-plane orientation to a canted state for a threshold electric field. Additional evidence for the spin flip has been obtained from data on the modulation of intensity of linearly polarized light due to diffraction by the stripe domains. A comprehensive theory for the voltage-induced magnetization flip is discussed and compared with the data. The magnetic transitions and the theory discussed here are of interests for electric-field-controlled magneto-optic and spintronic devices.

DOI: 10.1103/PhysRevB.87.134417 PACS number(s): 75.85.+t, 78.20.Ls, 77.84.−s, 75.70.Kw

I. INTRODUCTION

Spin-flip transitions associated with magnetic ordering in materials that are initiated by an external static magnetic field or temperature dependence of anisotropy fields are well known.[1–3] Meanwhile, there is another potential path for studies on such transitions: electric-field-induced modification of uniaxial anisotropy field in multiferroic composite materials.[4–9] The most promising multiferroics for such studies are magnetoelectric (ME) composites made by combining ferroelectric and ferro- or ferrimagnetic substances in which the ME response is orders of magnitude stronger than in single-phase ME materials at room temperature.[6] The ME effect in the mechanically bound two-phase composite materials is a product property arising from the magnetostriction and piezoelectric effects. In a ferrite-ferroelectric composite, for example, the static magnetization and high-frequency electromagnetic properties can potentially be controlled with an applied voltage.[4–14] Several recent studies reported experiments on electric-field-induced magnetization changes in ferromagnetic-piezoelectric ME systems, including magnetization reversal in ferrimagnetic nanopillars, magnetization rotation in Ni nanorings and nanobars, and changes in the magnetic anisotropy and stripe domain pattern modifications in Ni thin films.[10–14]

Bilayers of yttrium iron garnet, $Y_3Fe_5O_{12}$, and lead-zirconate-titanate (PZT) have been used extensively in the past for studies on the converse ME effects, i.e., voltage control of magnetic parameters in yttrium-iron-garnet (YIG).[6–9] Studies of significance in this regard include voltage tuning of M vs H_0, ferromagnetic resonance, and magnetoacoustic resonance.[6–9] A strong converse ME effect in YIG-PZT was inferred from these studies. A variety of novel voltage tunable ferrite devices, including microwave resonators, filters, phase shifters, and delay lines were demonstrated with the use of YIG-PZT.[6–9]

This work is on the optical observation and theory of magnetization flip due to an applied electric field in composites with single crystal thin films of YIG and polycrystalline PZT. Films of YIG in general are grown by liquid phase epitaxy (LPE) on gadolinium-gallium-garnet (GGG) substrates. Such films show an uniaxial anisotropy field, resulting in a specific type of stripe domain structure. LPE-grown YIG films are of particular interests due to excellent high-frequency magnetic properties.[15,16] Thin films are transparent in the visible region of the electromagnetic spectrum and show a large Faraday effect.[17] Magneto-optic techniques have been used in this study for the observation of (i) magnetic stripe domains with out-of-plane magnetization M_z in YIG and (ii) diffraction of light by the stripe domains when an electric field E is applied to PZT. With the application of a dc voltage V_0 across PZT, a gradual decrease in M_z is observed with increasing V_0 until a threshold voltage V_t when a first-order phase transition takes place with an abrupt change in the magnetization vector $\vec{M}$ to a canted state. The flip in the domain magnetization is a macroscopic analog of the well-known spin-flip phase transitions in ferrimagnetic and antiferromagnetic materials and is characterized by a stepwise rotation of $\vec{M}$ in individual domains instead of sublattices. For $V_0 > V_t$, the canting angle shows a gradual increase and a corresponding decrease in M_z. The changes in the domain magnetization are due to an E-induced uniaxial anisotropy in YIG that arises from piezoelectric deformation in PZT. A model for the effects has been developed, and theoretical estimates are in good agreement with the data.

This paper is organized as follows. Section II provides a theoretical description of voltage-controlled magnetic reorientation and spin-flip processes. Expressions are obtained for the stress-induced anisotropy fields and the free-energy density for the domain structure that depends on anisotropy fields. In Sec. III we discuss the choice of specific ferrite/piezoelectric metamaterial and details on the experimental setup. Section IV presents the experimental results on the voltage-induced reorientation and flip in magnetization vectors in the stripe domains. Also, results on polarized light diffraction by the stripe domain structure are presented, and the possibility of voltage control of transmitted light intensity and modulation

is demonstrated and discussed. Section V provides a summary and conclusion.

II. THEORY OF ELECTRIC-FIELD CONTROL OF DOMAIN MAGNETIZATION

A. Stripe domains and free energy

We consider the YIG film with stripe domains as in Fig. 1. The external static magnetic field H_0 is in the film plane and directed along the $[1\bar{1}0]$ axis. The surface normal is along [111], and with the $[11\bar{2}]$ direction completes the right-handed orthogonal coordinate system (Fig. 1). The domain walls are parallel to $\vec{H}_0$ and perpendicular to the sample surface. Such a model is fully consistent with the domain structure observed in our experiment (as discussed in detail later). The orientation of $\vec{M}$ in each domain (labeled $\vec{M}_1$ and $\vec{M}_2$) is specified by the respective azimuth and polar angles (ϕ_i, θ_i) in the spherical coordinate system whose polar axis coincides with the sample normal and the azimuth angle is measured from the $[11\bar{2}]$ direction. The equilibrium direction for the domain magnetization is determined by minimizing the free energy. Assuming the stripe domain structure to be periodic in the $[1\bar{1}2]$ direction, we estimate the free energy per unit volume as[18–22]

$$W = W_{an} + W_Z + W_{dd} + W_{dw},$$

where W_{an} is the crystalline anisotropy energy,[15] W_Z is the Zeeman energy, W_{dd} is the magnetic dipole-dipole energy that includes demagnetization energy for the net M of the sample and demagnetization energy of domain walls, and W_{dw} is the domain-wall energy.

The expression for free-energy density for the stripe domain structure is given by

$$\begin{aligned} W/M_0 = {} & \nu_1 H_{\rm cub}\left(\frac{1}{4}\cos^4\theta_1 + \frac{1}{3}\sin^4\theta_1 - \frac{\sqrt{2}}{3}\sin\theta_1\cos^3\theta_1\sin 3\phi_1\right) - \nu_1\frac{H_{U1}}{2}\sin^2\theta_1 - \nu_1\frac{H_{U2}}{4}\sin^4\theta_1 \\ & - \nu_1 H_0\cos\theta_1\sin\phi_1 + \nu_2 H_{\rm cub}\left(\frac{1}{4}\cos^4\theta_2 + \frac{1}{3}\sin^4\theta_2 - \frac{\sqrt{2}}{3}\sin\theta_2\cos^3\theta_2\sin 3\phi_2\right) \\ & - \nu_2\frac{H_{U1}}{2}\sin^2\theta_2 - \nu_2\frac{H_{U2}}{4}\sin^4\theta_2 - \nu_2 H_0\cos\theta_2\sin\phi_2 + 2\pi N_\perp M_0(\nu_1\sin\theta_1 + \nu_2\sin\theta_2)^2 \\ & + 2\pi N_{||} M_0(\nu_1\cos\theta_1\sin\phi_1 + \nu_2\cos\theta_2\sin\phi_2)^2 + 2\pi N_{dw}\nu_1\nu_2 M_0(\cos\theta_1\cos\phi_1 - \cos\theta_2\cos\phi_2)^2 \\ & + \frac{D}{S}\frac{M_0}{\pi^2}(\sin\theta_1 - \sin\theta_2)^2\sum_{n=1}\frac{1}{n^3}(1-\cos 2\pi n\nu_1) + \frac{2\gamma_{dw}}{M_0 D}, \end{aligned} \tag{1}$$

where $H_{\rm cub} = K_{\rm cub}/M_0$ is the cubic anisotropy field (note that for YIG: $K_{\rm cub} < 0$ and $H_{\rm cub} = -45$ Oe), $H_{U1} = 2K_{U1}/M_0$ and $H_{U2} = 4K_{U2}/M_0$ are the first- and second-order uniaxial anisotropy fields, respectively, M_0 is the saturation magnetization ($M_0 = 140$ G), $\gamma_{dw} = \gamma_{dw}(\varphi_i, \theta_i, K_{U1}, K_{U2}, K_{\rm cub}, D_{\rm ex})$ is the specific wall energy,[21] $N_\perp$ is the demagnetization factor in the perpendicular-to-plane direction ($N_\perp \approx 1$), $N_{||}$ is the in-plane demagnetizing factor in the direction parallel to H_0 ($N_{||} \ll 1$), $N_{dw} \approx S/(D+S)$ is the domain-wall demagnetization factor,[22] and $\nu_i = d_i/D$ is the volume of each part of the domain (in all of our calculations, the stripe domains are assumed to be equal in volume $\nu_1 = \nu_1 = 1/2$). The equilibrium state can be obtained by minimizing W with respect to the parameters θ_1, φ_1, θ_2, φ_2 for specific values of H_0 and H_{U1} and H_{U2}. Note that the last two terms in Eq. (1) include the domain period D, and these terms define the equilibrium domain width D_0. Indeed, while demagnetizing energy tends to make domains infinitely small, the accompanying increase in domain-wall energy prevents this, thereby stabilizing the domain period at some optimum value.[21] We will concentrate our attention on the region where the domain period remains constant.

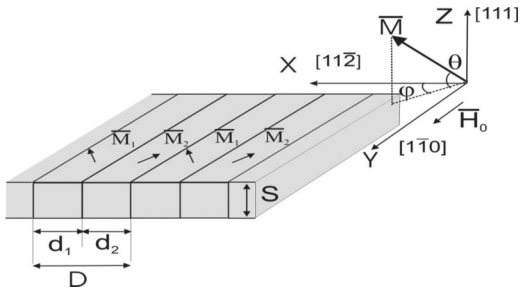

FIG. 1. Diagram showing the stripe domain structure in the yttrium-iron-garnet film, magnetic field, and magnetization directions assumed in the theory.

It is important here to discuss conditions under which the above model is valid. Obviously, the theory is applicable only when the domain structure corresponds to the structure in Fig. 1. As we have found out during experiments (discussed in Sec. III), for H_0 less than approximately 2 Oe, the periodic stripe domain is transformed into the labyrinth structure with the domains along three equivalent ⟨110⟩ directions in the film plane, with C_3 rotational symmetry about the [111] axis [as will be seen in Fig. 5(a)]. This lower boundary is defined by the energy barrier between adjacent ⟨110⟩ directions, namely, the energy difference between the ⟨110⟩ and ⟨112⟩ axes. On the high-field side, when H_0 exceeds approximately 8 Oe, domains become substantially unequal in width, with the energetically favorable one prevailing. This can also be observed by the

appearance of the even maxima in the diffraction pattern [Fig. 5(c)], as discussed later. We can set the high-field limit according to $d_2/d_1 > 1.1$, assuming d_2 is for the energetically favorable domain.

B. Theory of electric-field-induced anisotropy

Next, we consider magnetoelastic energy of YIG film grown on GGG. The energy is a function of strain tensor ε_{ij}, direction cosines of magnetization α_i, and direction cosines of the normal to the substrate β_i.[23] The exact form of this phenomenological expression is determined by the crystal symmetry. It was found that for ferrites with cubic symmetry grown on the (111) substrate ($\beta_i = 1/\sqrt{3}$), energy could be represented as[24]

$$W_{me} = -K^E_{U1}\alpha_z^2 + K^E_{\text{cub}}\left(\alpha_1^2\alpha_2^2 + \alpha_2^2\alpha_3^2 + \alpha_1^2\alpha_3^2\right) - K^E_{U2}\alpha_z^4, \tag{2}$$

where $K^E_{U1} = 3b_2\varepsilon_a - 3b_4\varepsilon - \frac{3}{2}b_5\varepsilon_a$, $K^E_{U2} = \frac{9}{4}b_5\varepsilon_a$, $K^E_{\text{cub}} = 3(b_3 + \frac{2}{3}b_4)\varepsilon - b_5\varepsilon_a$, $\varepsilon_a = \sigma/(3c_{44})$, $\varepsilon = (\sigma/(c_{11} - c_{12}))\cdot(1/3 - c_{12}/(c_{11} + 2c_{12}))$, α_z is a direction cosine with respect to the $\langle 111\rangle$ axis, c_{ij} being YIG stiffness constants, b_i is the magnetoelastic coupling coefficients, and σ is the mechanical stress applied along the surface normal. Equation (2) has the classical form of mixed (cubic and uniaxial) magnetocrystalline anisotropy energy, and hence the coefficients $K^E_{U1}(\sigma)$, $K^E_{U2}(\sigma)$, and $K^E_{\text{cub}}(\sigma)$ have physical meaning of the stress-induced anisotropy constants (first- and second-order uniaxial and first-order cubic, respectively).[15] Consequently, magnetocrystalline anisotropy energy constants and fields in YIG films should be treated as comprising two parts, for instance, $H_{U1} = H^0_{U1} + H^E_{U1}(\sigma)$, where H^0_{U1} is the growth-induced anisotropy.[23] The origin of the perpendicular magnetic anisotropy is the growth-induced strain at the film-substrate interface and arises due to two factors: (i) slight mismatch in the lattice constants of the GGG substrate and the YIG film, and (ii) the difference in the thermal expansion coefficients of GGG and YIG. The term $H^E_{U1}(\sigma)$ is due to the (E-field-) induced piezoelectric strain term. Assuming $b_3, b_4, b_5 \ll b_1, b_2$, we can neglect $K^E_{U2}(\sigma)$ and $K^E_{\text{cub}}(\sigma)$ and obtain the well-known expression[25–27]

$$K^E_{U1}(\sigma) = \frac{b_2\sigma}{c_{44}} = -\frac{3}{2}\lambda_{111}\sigma, \tag{3}$$

where $\lambda_{111} = -2b_2/(3c_{44})$ is the magnetostriction constant.[28]

In the case of a YIG-PZT composite structure, voltage-induced mechanical stress in YIG could be expressed as $\sigma = (E/(1-\nu))\cdot(V_0/S)\cdot d_{31}$, where E is Young's modulus ($E = 2\cdot 10^{11}$ Pa for YIG[28]), ν is the Poisson's ratio ($\nu = 0.29$), $d_{31} = -2.7\cdot 10^{-10}$ m/V is the piezoelectric coefficient for PZT, V_0 is the applied voltage, and S is the PZT thickness. Therefore, we obtain

$$H^E_{U1}(V_0) = \frac{2K_{U1}}{M_0} = -\frac{3E}{1-\nu}\frac{\lambda_{111}}{M_0}\frac{d_{31}}{S}V_0. \tag{4}$$

Hence, the ME effect in the layered ferrite-piezoelectric structure manifests as voltage-induced generation of the first-order unaxial anisotropy field in the ferrite film.[5] Since the electric field induces piezoelectric strain in PZT that is transferred to YIG and GGG, the overall uniaxial anisotropy field in YIG will depend critically on the thickness of both the YIG and GGG. For a given E-value, one anticipates a decrease in the anisotropy field with increasing YIG film thickness.

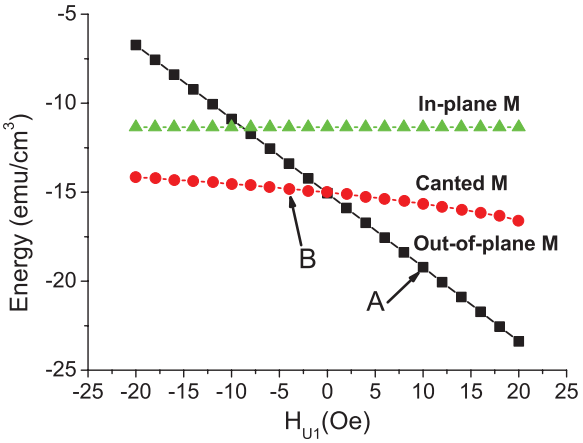

FIG. 2. (Color online) Equilibrium energy of domain magnetization states, i.e., out-of-plane, in-plane, and canted states, as a function of uniaxial anisotropy field. A and B correspond to regions of antiparallel and canted domain magnetization states (as in Fig. 3).

C. Voltage-controlled magnetization flip

Minimization of the energy density [Eq. (1)] revealed the presence of three different local energy minima, namely, the out-of-plane (OOP, $\theta_1 \approx \pi/2$, $\theta_2 \approx -\pi/2$), the in-plane (IP, $\theta_1 \approx 0$, $\theta_2 \approx 0$), and the canted state ($\theta_1 \approx \theta_c$, $\theta_2 \approx -\theta_c$, $0 < \theta_c < \pi/2$, and θ_c depends on H_0 and H_{U1} values).

In order to determine the influence of the uniaxial anisotropy field on the equilibrium domain structure, we calculated the dependence of energy of these three states on H_{U1} for $M = 140$ G, $H_{\text{cub}} = -45$ Oe, and $H_0 = 4$ Oe. We assumed the second-order anisotropy field $H_{U2} = -H_{U1}/3$.[29] Note that H_{U1} should be treated as a total uniaxial anisotropy field, consisting of growth-induced H^0_{U1} and electric-field-induced $H^E_{U1}(V_0)$ parts. The domain energy is plotted as a function of H_{U1} in Fig. 2. It is seen in Fig. 2 that for the positive uniaxial field, the domain magnetization is oriented predominantly along the surface normal (OOP state), while with decreasing H_{U1}, the magnetization experiences a transition to a canted configuration. In this phase θ_c changes from 17° to 23° for H_{U1} from -10 Oe to 10 Oe, and the out-of-plane component of magnetization $M^z_{1,2} = |M_0 \sin\theta_{1,2}|$ is in the range 41–55 G. The perpendicular magnetization is of specific interest because it is the component that determines the Faraday rotation and, thus, is detected in our magneto-optic experiments. Since the regions of stability of magnetic phases under consideration overlap, this is a first-order magnetization-flip phase transition.[1] It is demonstrated in Fig. 3 where the energy for the perpendicular-to-plane magnetization state is depicted as a function of applied voltage. Here $H^E_{U1}(V_0)$ was calculated using Eq. (4) and the measured material parameters. In order to account for ferroelectric hysteresis in PZT, we have expanded the phase transition point into a finite-width region. Previous microwave experiments facilitated direct measurements of $H^E_{U1}(V_0)$ hysteresis, showing an average

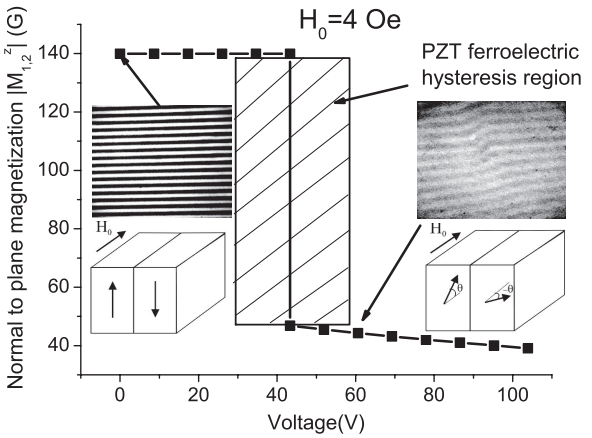

FIG. 3. Out-of-plane component of equilibrium magnetization vs applied voltage. H^0_{U1} is assumed to be 10 Oe. Magneto-optical images of domain structure before and after magnetization flip to canted structure are also shown.

width of roughly 30 V.[5] That value was transferred onto the hysteresis region in Fig. 3.

To summarize, if the initial growth-induced uniaxial anisotropy of magnetic film is rather small ($|H_{U1}| < 10$ Oe), one can cause drastic modification of the equilibrium magnetization orientation with the application of a voltage (and a stress-induced uniaxial anisotropy field). Thus, the possibility for substantial electric field control of magnetic domain structure arises.

III. EXPERIMENT

The experimental setup for the observation of the domain structure and corresponding diffraction pattern in polarized light is presented in Fig. 4. The intensity of the diffracted light and the Faraday rotation of nondiffracted light were measured with a photodetector for quantitative characterization of the domain structure transformation. In this experiment, YIG film was bonded to a PZT disk with a diameter of 10 mm and thickness of 0.2 mm. The PZT disk had silver electrodes, was poled by heating to 320 K and cooling in $E_0 = 20$ kV/cm. A 2-mm-diameter hole was drilled in the disk to provide transmission of light. YIG films of 10 μm in thickness

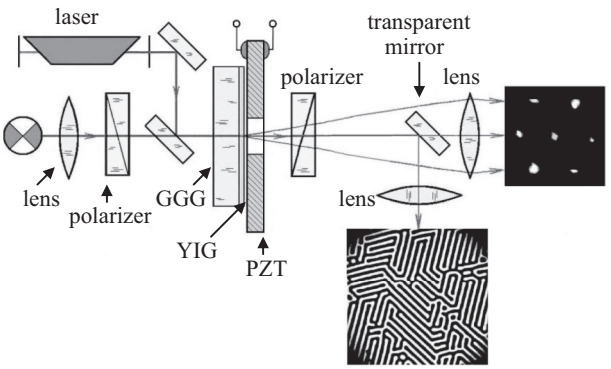

FIG. 4. Schematic diagram showing the experimental setup for magneto-optical measurements, imaging of domain structure, and diffraction pattern for YIG-PZT.

on 0.5-mm-thick GGG substrates were used. As mentioned earlier in Sec. I, the YIG thickness S must be much smaller than PZT and GGG thickness for best strain transfer and desired voltage-induced uniaxial anisotropy. From available YIG films, we chose the one with the lowest crystallographic uniaxial anisotropy field, $H^0_{U1} = +8$ Oe. In this situation, the effect of voltage-induced anisotropy should be the most distinct.

IV. RESULTS AND DISCUSSION

A. Voltage-induced magnetization-flip phase transition

In the absence of any voltage or bias magnetic field applied to PZT, the YIG film showed irregular labyrinth domain structure as in Fig. 5(a). When a magnetic field H_0 of several Oe was applied in the film plane parallel to [110], stripe domains lined up along [110] appeared as shown in Fig. 5(b). Further increase in H_0 led to the increase in width of energetically favorable domains, while the total period changed only slightly as in Fig. 5(c). Finally, for $H_0 \geqslant H_{\text{cub}}$, the film reached magnetically saturated state.

It was found that a voltage applied to PZT can cause transitions involving flip of domain magnetization from perpendicular to canted structure or vise versa. For instance, the YIG film when subjected to $H_0 = 4$Oe shows stripe domains with the out-of-plane magnetization, as clearly seen in Fig. 5(b). When a voltage $V_0 = 60$ V is applied across PZT, the domain pattern deteriorates, as in Fig. 5(d), implying that the static magnetization in the domains is now inclined with respect to film plane. When the polarity of voltage is changed, the domain structure remains the same, but the magnetic field required for reorientation of magnetization somewhat increased.

The domain structures in Fig. 5 are as expected from the theoretical considerations in Sec. II. Indeed, the voltage applied to the PZT platelet causes a compressive or tensile stress (depending on the voltage polarity), which is transferred to the YIG via mechanically rigid bonding and creates stress-induced first-order uniaxial anisotropy field in accordance with Eq. (4). This field adds on to the uniaxial anisotropy field and, according to Eq. (1) and Fig. 2, results in modification of the equilibrium domain structure. It was found that for $H_0 = 4$ Oe the magnetization flip occurs for $V_0 = 40$ V. From Eq. (4), we calculated $H^E_{U1}(V_0) = -9.2$ Oe, implying a total field $H_{U1} = H^0_{U1} + H^E_{U1}(V_0) = -1.2$ Oe, that is rather close to theoretical value $H_{U1} = -0.5$ Oe (see Fig. 2). The larger magnitude of H_0 domains become unequal in width, the model is no longer valid, and calculated values deviate from experiment.

B. Voltage modulation of transmitted light intensity

Further evidence for the electric-field-induced magnetization-flip transition was obtained through studies on modulation of the intensity of light transmitted through the film. The YIG film with a periodic stripe domain structure is essentially a grating that formed a diffraction pattern showing interference maxima, located in the transverse direction (which is $[11\bar{2}]$ in our case) as shown in Fig. 5. The intensity

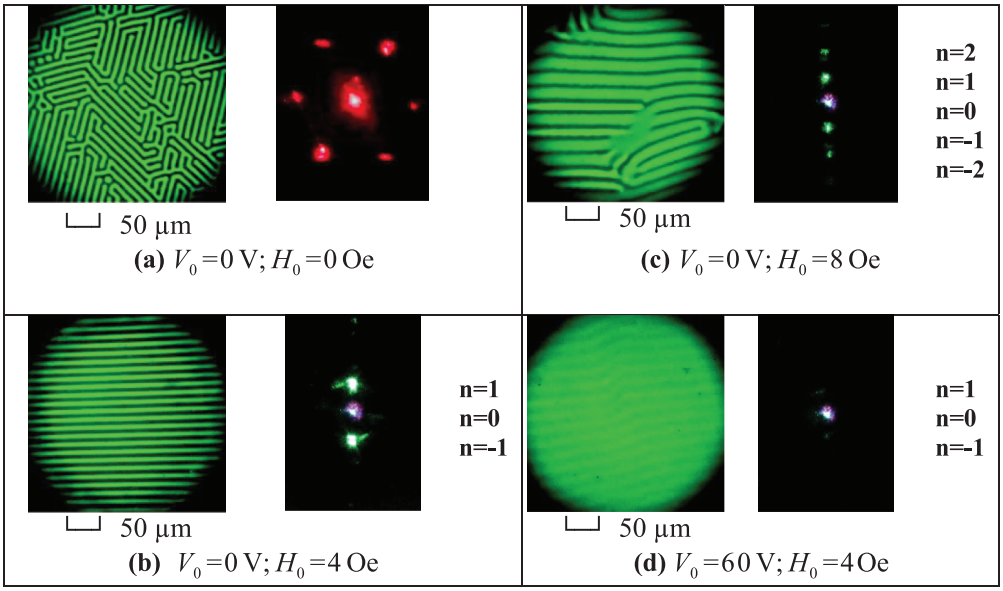

FIG. 5. (Color online) (a)–(c) Evolution of YIG domain structure and diffraction pattern under the influence of external magnetic field; (d) voltage-induced magnetization flip. n denotes the diffraction order. The bias magnetic field is directed from left to right.

of the first interference maximum is given by

$$I_1 = I_0 \frac{4}{\pi^2} \cdot \sin^2(\phi_F \cdot M_z S) \cdot e^{-\alpha S}, \tag{5}$$

where I_0 is the intensity of a light beam entering the film, S is the thickness of the YIG film, $\alpha = 620$ cm^{-1} is the absorption coefficient at $\lambda = 628$ nm, and $\varphi_F = 0.89 \cdot 10^{-3}$ deg/(μm·G) is the angle of specific Faraday rotation in YIG. The relative intensity of the first maximum I_1/I_0 for YIG film is rather small, with no more than 0.01% in the 633-nm range and 0.02% in the 425-nm range. However, it is sufficient for direct observations and quantitative measurements. In YIG films doped with bismuth, diffraction efficiency rises, and I_1/I_0 can reach 1% since the specific Faraday rotation for pure bismuth iron garnet at a wavelength of 633 nm is two orders of magnitude larger than in pure YIG.[30]

At first, we investigated the intensity of the first diffraction maximum as a function of dc bias voltage V_0 at $H_0 = 4$ Oe, and the results are presented in Fig. 6 (after background signal subtraction). One can see a clear hysteresis in the intensity and $I_{\max}/I_{\min} \sim 10.5$ and modulation depth $(I_{\max} - I_{\min})/(I_{\max} + I_{\min}) = 82\%$. The data are also direct evidence of magnetization-flip transition, which implies that for large negative voltage, the perpendicular component of magnetization in domains is appreciably smaller than at zero bias. Moreover, using Eq. (5), we can roughly estimate the magnitude of M_z in canted state. We estimate from the data that $M_z = 43$ G, which is rather close to theoretical predictions (see Fig. 3).

There is qualitative agreement between the change in the diffracted intensity with bias voltage shown in Fig. 6 and the anticipated electric-field dependence of strain in PZT. The piezoelectric strain in PZT increases with increasing voltage, which, in turn, changes the magnetization direction and the domain structure. Far from the spin-flip region, any change in the magnetization direction is rather small, and the diffraction intensity does not show measurable dependence on the bias voltage. For voltages high enough to cause the spin-flip transition from one domain structure to another, the diffracted intensity changes abruptly. Theoretical estimates of the voltages using the strain-induced uniaxial anisotropy model are in agreement with the data.

In order to investigate the voltage induced magnetization flip and the resulting modulation of light, we applied $H_0 = 1$ Oe and a dc voltage V_0 large enough to achieve a domain structure close to the magnetization-flip point. Then, we applied an ac voltage of meander shape and measured the time-dependent intensity of diffraction maxima, and the data are presented on Fig. 7. One can see that sufficiently large voltage variation (peak-to-peak value V_{pp} was taken, 16 V) leads to periodic rearrangement of the static magnetization in the domain structure, resulting in periodically varying intensity of the diffraction light. Indeed, for the OOP magnetization case, domains effectively act as a diffraction grating, and diffraction

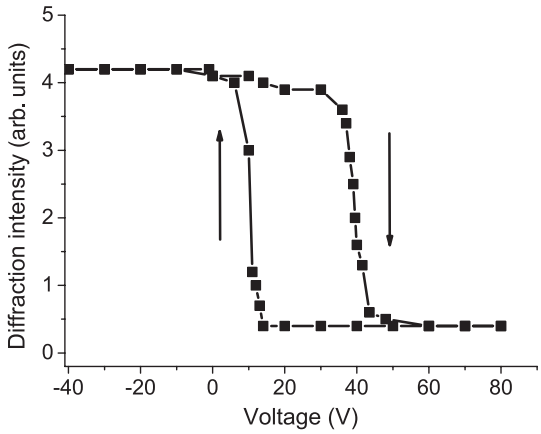

FIG. 6. Data showing the first-order diffraction intensity maximum vs voltage V_0 for $H_0 = 4$ Oe.

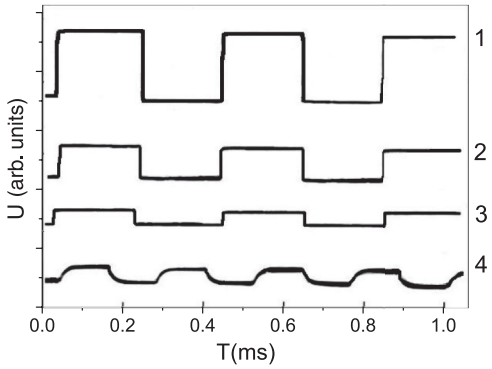

FIG. 7. Oscillograms of the diffraction intensity modulation by means of ac voltage, applied to PZT: $1 - V_0 = 54$ V, $f = 2.5$ kHz; $2 - V_0 = 64$ V, $f = 2.5$ kHz; $3 - V_0 = 74$ V, $f = 2.5$ kHz; $4 - V_0 = 54$ V, $f = 4$ kHz. Bias magnetic field $H_0 = 1$ Oe.

maximum intensity is registered; for canted orientation the light passes through grating with much lower contrast [due to $\sin 2(\varphi_F \cdot M_z S)$ term in Eq. (5)] and the detector, placed in the position of first maximum, records a much smaller signal. Figure 7 shows the shape of output signal, which was almost identical to the shape of input one. Values of both the dc and pulsed voltages for light modulation can be drastically reduced if thinner piezoelectric layer could be used. For example, a 40-μm-thick PZT will require five times smaller operating voltage.

Amplitude and shape of output signal remains steady for input signal frequencies f from 0 to 3 kHz. Further frequency increase leads to the progressive distortion and gradual decrease of modulation amplitude for $f > 3$ kHz that eventually falls down to almost zero at $f = 5$ kHz. Figure 7 showing the output signal measured at $f = 4$ kHz illustrates this point and could be associated with acoustic modes in the sample as discussed below.

The radial acoustic mode frequency for the 10-mm-diameter PZT used in this study is of the order of 6 kHz. Our experiments indicate substantial energy dissipation and sample heating when the modulation frequency is tuned to the resonance frequency. According to the data presented in Fig. 7, for modulation frequencies above 4 kHz, the shape of the intensity profiles become more and more distorted (Fig. 7, curve 4, for example), and the amplitude of modulation decreases until it decreases to zero. It is quite possible that such behavior is due to sample heating for frequencies close to the resonance frequency of whole PZT/YIG/GGG structure. Further studies are necessary to resolve this question.

Finally, it is also of interest to measure the M vs H_0 for the composite under an electric field to confirm the magnetization flip observed by optical techniques in this study. The flip is expected to alter the shape of the M vs H_0 loop upon the application of an electric field to PZT,[6] but our preliminary studies did not show any measurable variation in the M vs H_0 characteristics. Establishing a correlation between M vs H_0 under an applied voltage and the domain structure in Fig. 4 is a subject of interest for further investigation.

V. CONCLUSION

Electric-field control of the domain magnetization state has been studied in a bilayer of YIG and PZT. Both the domain observation by the Faraday effect and light diffraction measurements have been utilized to demonstrate the magnetization flip to a canted state upon the application of a dc voltage across PZT. The resulting piezoelectric strain manifests as the uniaxial anisotropy field in YIG and leads to the spin flip for a threshold voltage. The magnetization flip to the canted state is inferred from the change in the domain structure and the intensity of diffracted light. A theory that describes the magneto-optically observed magnetization-flip transition is presented. Theoretical estimates for the magnetization-flip voltage agree with experimentally measured values within the range of uncertainty due to ferroelectric hysteresis in PZT. The theory developed here is valid for any ferrite-piezoelectric composite for estimates on the respective magnetization state. The results presented here are of interest for electric-field control of magneto-optical and spintronic devices.

ACKNOWLEDGMENT

The efforts at Oakland University were supported by the National Science Foundation (Grant No. DMR-0902701).

[1] V. G. Bar'yakhtar, V. A. Borodin, V. D. Doroshev, N. M. Kovtun, R. Z. Levitin, and E. P. Stefanovskii, Sov. Phys. JETP **47**, 315 (1978).
[2] R. E. Bornfreund, D. C. Khan, P. E. Wigen, M. Parvadi-Horvath, J. B. Ings, and R. F. Belt, J. Magn. Magn. Mater. **151**, 181 (1995).
[3] A. V. Bezus, A. A. Leonov, Yu. A. Mamalui, and Yu. A. Siryuk, Phys. Solid State **46**, 283 (2004).
[4] C.-W. Nan, M. I. Bichurin, D. Viehland, S. Dong, and G. Srinivasan, J. Appl. Phys. **103**, 031101 (2008).
[5] M. A. Popov and I. V. Zavislyak, Tech. Phys. Lett. **38**, 865 (2012).
[6] N. X. Sun and G. Srinivasan, SPIN **2**, 1240004 (2012).
[7] C. Pettiford, S. Dasgupta, Jin Lou, S. D. Yoon, and N. X. Sun, IEEE Trans. Magn. **43**, 3343 (2007).
[8] G. Srinivasan, A. S. Tatarenko, Y. K. Fetisov, V. Gheevarughese, and M. I. Bichurin, in *MRS Proceedings*, Vol. 966 (Materials Research Society, Warrendale, 2006), p. 0966-T14-01.
[9] V. Petrov, G. Srinivasan, O. V. Ryabkov, S. V. Averkin, and M. I. Bichurin, Solid State Commun. **144**, 50 (2007).
[10] F. Zavaliche, T. Zhao, H. Zheng, F. Straub, M. P. Cruz, P.-L. Yang, D. Hao, and R. Ramesh, Nano Lett. **7**, 1586 (2007).
[11] Tien-Kan Chung, S. Keller, and G. P. Carman, Appl. Phys. Lett. **94**, 132501 (2009).
[12] J. L. Hockel, A. Bur, T. Wu, K. P. Wetzlar, and G. P. Carman, Appl. Phys. Lett. **100**, 022401 (2012).
[13] T. Wu, A. Bur, P. Zhao, K. P. Mohanchandra, K. Wong, K. L. Wang, C. S. Lynch, and G. P. Carman, Appl. Phys. Lett. **98**, 012504 (2011).

[14]Chin-Jui Hsu, J. L. Hockel, and G. P. Carman, Appl. Phys. Lett. **100**, 092902 (2012).
[15]I. V. Zavislyak and M. A. Popov, in *Yttrium: Compounds, Production and Applications*, edited by B. D. Volkerts (Nova Science Publishers, Inc., New York, 2011), p. 278.
[16]M. I. Bichurin and D. Viehland, *Magnetoelectricity in Composites*, (Pan Stanford Publishing, Singapore, 2011), p. 286.
[17]T. Aichele, A. Lorenz, R. Hergt, and P. Görnert, Cryst. Res. Technol. **38**, 575 (2003).
[18]J. O. Artman, Phys. Rev. **105**, 62 (1957).
[19]S. A. Kirov, A. I. Pilshchikov, and N. E. Syryev, Fiz. Tverd. Tela (Leningrad) **16**, 3051 (1974).
[20]Yu. V. Gulyaev, P. E. Zil'berman, R. J. Elliott, and E. M. Epshtein, Phys. Solid State **44**, 1111 (2002).
[21]A. Hubert and R. Schäfer, in *Magnetic Domains* (Springer-Verlag, Berlin, 2009), p. 686.
[22]T. E. Hasty, J. Appl. Phys. **35**, 1434 (1964).
[23]H. Szymczak and N. Tsuya, Phys. Status Solidi A **54**, 117 (1979).
[24]M. A. Popov and I. V. Zavislyak, in *22nd International Crimean Conference on Microwave and Telecommunication Technology (CriMiCo)* (IEEE, Sevastopol National Technical University, Sevastopol, Ukraine, 2012), pp. 593–594.
[25]A. B. Smith and R. V. Jones, J. Appl. Phys. **34**, 1283 (1963).
[26]B. Hoekstra, F. van Doveren, and J. M. Robertson, Appl. Phys. **12**, 261 (1977).
[27]M. Kubota, A. Tsukazaki, F. Kagawa, K. Shibuya,Y. Tokunaga, M. Kawasaki, and Y. Tokura, Appl. Phys. Express **5**, 103002 (2012).
[28]Yu. M. Yakovlev and S. Sh. Gendelev, in *Ferrite Monocrystals in Radio Eelectronics* (Soviet-era, Moscow, 1975), p. 360 [in Russian].
[29]P. R. T. Pugh, J. G. Booth, J. W. Boyle, J. A. Cowen, A. D. Boardman, I. Zavislyak, V. Bobkov, and V. Romanyuk, J. Magn. Magn. Mater. **196–197**, 498 (1999).
[30]T. Okuda, N. Koshizuka, K. Hayashi, H. Kobani, and H. Yamamoto, IEEE Trans. Magn. **5**, 3491 (1987).